

Interaction between point charges, dipoles and graphene layers

Francisco Guinea^{1,2,*} and Niels R. Walet^{1,†}

¹*Theoretical Physics Division, School of Physics and Astronomy,
University of Manchester, Manchester M13 9PL, UK*

²*IMDEA Nanoscience, C/Faraday, 9 Ciudad Universitaria de Cantoblanco 28049, Madrid, Spain*

We analyse the interaction between charges and graphene layers. The electric polarisability of graphene induces a force, that can be described by an image charge. The analysis shows that graphene can be described as an imperfect conductor with a finite dielectric constant, ϵ_r , for weak coupling, and it behaves as a metal for strong fields. As a consequence, the interaction between polar molecules and graphene layer(s) tends to align the molecular dipole along the direction normal to the graphene, and quantitative estimates of the energy gain are given. The strength of this interaction can be sufficient to overcome thermal effects when the molecule is close to the layer, even at room temperature. Hence, boundary effects play a significant role in determining the structure of systems such as water confined in atomically narrow van der Waals heterostructures.

PACS numbers: 68.65.Pq, 74.25.N-

I. INTRODUCTION

Advances in the design of van der Waals heterostructures¹ have lead to the confinement of a number of substances between graphene layers^{2–5}. The materials between the layers can experience large pressures, which can lead to changes in their structure. The properties of matter under such extreme pressure has been extensively studied using techniques such as the Density Functional Theory^{6,7}, DFT, which can give a good approximation to the ground state energy, and makes it possible to compare different structures. As a recent example, consider the description of superconducting hydrogen sulfide under pressure, e.g., Ref.^{8–10}, where density functional theory is used extensively to describe the behaviour of bulk systems.

Most theoretical work on matter under high pressure has focused on such bulk properties, without considering the role played by the boundary conditions at the surface of the system. Matter confined in van der Waals heterostructures is in close contact with the layers in which it is embedded. The influence of the boundary conditions on the total energy is, most likely, comparable to or even exceeds the bulk contribution. Moreover, graphene is a semimetal, which can interact with electric charges and dipoles in the confined material. This gives rise to image charge forces that are difficult to implement in standard DFT calculations, although simple electrostatic arguments can give a reasonable estimate. For example, most recent computational work on water confined between graphene uses a simple surface integrated van der Waals (3-9) force to describe the water-graphene interaction^{11,12}, which is, at best, a crude approximation, since it ignores the image charges caused by the semi-metal. There is substantial work where the water-graphene interaction is described fully microscopically^{13–18}, but such approaches, although very insightful, seem of limited practical use in complex calculations. It would thus be quite interesting to see whether we can find a better effective model for the long-range behaviour of the interaction between charges and graphene.

In the following, we focus on the dipolar interactions between water molecules and graphene layers. There are approaches where the graphene and water are both described by density-functional theory with van der Waals dispersive forces, e.g., Ref.¹⁹. As such calculations are very complex, and thus have only limited reach, we would like to generate models that include such interactions in a more approximate way, so that we can concentrate on the behaviour of the confined molecules without the additional complication of having to describe the detail of the graphene. To that end we study the effect of charges on graphene layers and bilayers using two approximations, linear response and the Thomas-Fermi method. These methods are quite general, and can be applied to other dipolar molecules and confining layers. We first study the screening of a point charge and a dipole outside a single graphene layer. The results are generalized to a dipole between two layers in section III. In section IV we present quantitative estimates for the interaction of a water molecule within a graphene bilayer, as function of the orientation of the molecule. Some details of the calculations are discussed in the Appendix.

II. SINGLE (FLAT) LAYER

We first consider the interaction of a point charge with a single graphene layer. We assume that the charge is at a distance z from the layer. The potential induced by the charge on the graphene layer, $V(\mathbf{r}_{\parallel}, z) = Ze^2/\sqrt{|\mathbf{r}_{\parallel}|^2 + z^2}$ reduces to the Coulomb potential at distances $|\mathbf{r}_{\parallel}| \gg z$. The screening of a point charge in graphene was treated in detail in²⁰. The effective fine structure constant of graphene, $\alpha_G = e^2/(4\pi\epsilon_0\hbar v_F) = Z\alpha c/v_F$, allows us to define two regimes, depending on whether $Z\alpha_G \lesssim 1$ or $Z\alpha_G \gtrsim 1$ ^{21,22–26}. We treat separately the cases $Z\alpha_G \ll 1$ (perturbative regime) and $Z\alpha_G \gg 1$ (strong coupling).

A. RPA screening: Subcritical regime, $Z\alpha_G \ll 1$

1. Point charge

In the subcritical regime, where the effective coupling parameter $Z\alpha_G \ll 1$, we can use linear response to find the additional potential induced by a charge placed near a graphene layer. Specifically, consider a point charge Ze displaced with respect to the origin a distance $\mathbf{r}_{\parallel 0}$ parallel to the layer, and a distance z_0 from the layer in the perpendicular direction. We assume that the layer is infinitesimally thin, so that its polarisability can be described by the equation

$$\chi(\mathbf{r}_{\parallel}, z) = \chi(\mathbf{r}_{\parallel})\delta(z), \quad (1)$$

where we assign the graphene layer the coordinate $z = 0$. The potential inside the graphene layer by the charge is $V_0(\mathbf{r}_{\parallel}, 0) = V_{\text{Coulomb}}(\mathbf{r}_{\parallel} - \mathbf{r}_{\parallel 0}, z_0)$, but this is screened due to the induced charge density inside the layer,

$$V_{\text{scr}}(\mathbf{r}_{\parallel}, z) = \frac{e^2}{4\pi\epsilon_0} \int d^2\mathbf{s} \frac{1}{\sqrt{|\mathbf{r}_{\parallel} - \mathbf{s}|^2 + z^2}} \chi(\mathbf{r}_{\parallel} - \mathbf{s}) V_{\text{tot}}(\mathbf{s}, 0), \quad (2)$$

where $V_{\text{tot}} = V_0 + V_{\text{scr}}$. This can easily be evaluated in the von Laue coordinates $(\mathbf{q}_{\parallel}, z)$

$$V_{\text{scr}}(\mathbf{q}_{\parallel}, z) = \frac{1}{2\epsilon_0 q_{\parallel}} e^{-q_{\parallel} z} \chi(\mathbf{q}_{\parallel}) V_{\text{tot}}(\mathbf{q}_{\parallel}, 0). \quad (3)$$

The polarisability of graphene in the RPA approximation is²⁷

$$\chi(\mathbf{q}_{\parallel}) = -\frac{n_f}{32} \frac{q_{\parallel}}{\hbar v_F}, \quad (4)$$

where v_F is the Fermi velocity in the graphene layer, and $n_f = 4$ is the number of fermion flavours in graphene. Making a 2D Fourier transform of the Coulomb potential, we find

$$\begin{aligned} V_0(\mathbf{q}_{\parallel}, 0) &= V_{\text{Coulomb}}(\mathbf{q}_{\parallel}, z_0) \\ &= Ze^2 \frac{1}{2\epsilon_0 q_{\parallel}} e^{i\mathbf{q}_{\parallel} \cdot \mathbf{r}_{\parallel 0}} e^{-q_{\parallel} |z_0|}. \end{aligned} \quad (5)$$

Assuming $z_0 > 0$, we now solve for the in-layer screening potential $V_{\text{scr}}(\mathbf{q}_{\parallel}, 0)$, using the shorthand $x_{\text{RPA}} = e^2/16\epsilon_0\hbar v_F = \frac{\pi}{4}\alpha_G$,

$$\begin{aligned} V_{\text{scr}}(\mathbf{q}_{\parallel}, 0) \left(1 - \frac{1}{2\epsilon_0 q_{\parallel}} \chi(\mathbf{q}_{\parallel})\right) &= \frac{1}{2\epsilon_0 q_{\parallel}} \chi(\mathbf{q}_{\parallel}) V_0(\mathbf{q}_{\parallel}, 0), \\ V_{\text{scr}}(\mathbf{q}_{\parallel}, 0) &= -\frac{x_{\text{RPA}}}{1 + x_{\text{RPA}}} Z \frac{e^2}{2\epsilon_0 q_{\parallel}} e^{i\mathbf{q}_{\parallel} \cdot \mathbf{r}_{\parallel 0}} e^{-q_{\parallel} z_0}. \end{aligned} \quad (6)$$

We can use this in turn to work out the general potential,

$$\begin{aligned} V_{\text{scr}}(\mathbf{q}_{\parallel}, z) &= \frac{1}{2\epsilon_0 q_{\parallel}} e^{-q_{\parallel} z} \chi(\mathbf{q}_{\parallel}) V_{\text{tot}}(\mathbf{q}_{\parallel}, 0) \\ &= e^{-q_{\parallel} z} V_{\text{scr}}(\mathbf{q}_{\parallel}, 0). \end{aligned} \quad (7)$$

Thus, finally, transforming to coordinate space,

$$\begin{aligned} V_{\text{scr}}(\mathbf{r}_{\parallel}, z) &= \frac{x_{\text{RPA}}}{1 + x_{\text{RPA}}} \frac{Ze^2}{4\pi\epsilon_0} \int dq_{\parallel} J_0(q|\mathbf{r}_{\parallel} - \mathbf{r}_{\parallel 0}|) e^{-q_{\parallel}(z_0+z)} \\ &= \frac{x_{\text{RPA}}}{1 + x_{\text{RPA}}} \frac{Ze^2}{4\pi\epsilon_0} Ze^2 \frac{1}{(|\mathbf{r}_{\parallel} - \mathbf{r}_{\parallel 0}|^2 + (z + z_0)^2)^{1/2}}. \end{aligned} \quad (8)$$

This is just the effect of an imperfect image charge: in the metallic limit ($x_{\text{RPA}} \rightarrow \infty$) we find that the screening potential is equal but opposite to the applied potential, and in the vacuum limit ($x_{\text{RPA}} = 0$) we have no screening at all. Thus, using the results in, e.g., Ref.²⁸, we see that we can identify

$$\frac{x_{\text{RPA}}}{1 + x_{\text{RPA}}} = \frac{\epsilon_r - 1}{\epsilon_r + 1}, \quad (9)$$

or more simply

$$\epsilon_r = 1 + 2x_{\text{RPA}}. \quad (10)$$

2. Point dipole

Since the dominant interaction of a polar but electrically neutral molecule placed in front of a graphene will be caused by the dipole force it is interesting to look at the simplified case of a point dipole.

We consider such a point-dipole with dipole moment D at the point $r_{\parallel} = 0$, $z = z_0$, and the dipole moment making an angle θ with respect to the normal to the graphene layers. The effect of the screening interaction leads to an effective potential energy for the dipole, which orients the dipole perpendicular to the surface,

$$V_{\text{Dipole}} = -\frac{\epsilon_r - 1}{\epsilon_r + 1} \frac{D^2(1 + \cos^2 \theta)}{32\pi\epsilon_0 z_0^3}. \quad (11)$$

This agrees with the qualitative statement (see, e.g., Ref.²⁹) that water molecules orient preferentially perpendicular to the graphene layers.

B. Strong coupling

The RPA analysis, based on linear response theory, is valid for $Z\alpha_G \ll 1$. The effect of a charged impurity, Ze , on a graphene layer shows a transition to a strong coupling regime, the supercritical regime, for $Z\alpha_G \sim 1$ ^{22–26}. In this regime, the induced potential creates resonances within the graphene band, and linear response theory is no longer applicable.

Let us first consider the extreme case $Z\alpha_G \gg 1$. The potential near the external charge changes slowly with distance over distances $r \sim d$. The induced charge density in the graphene layer, $\rho \sim Z\alpha_G/d^2$, also changes slowly with r , and leads to a screening length²² $k_{\text{TF}}^{-1} \sim d/(Z\alpha_G) \ll d$. This allows us to use the Thomas-Fermi approximation^{20,30}. In this approximation the total energy of the graphene layer can be expressed in terms of the induced electron number density $\rho(\mathbf{r})$. This is defined relative to the background density, so this can be positive or negative, but

we find that $\text{sign}(Z)\rho$ is positive. Thus

$$\begin{aligned} E_{\text{TF}} &= E_{\text{kin}} + E_{\text{pot}} + E_{\text{int}}, \\ E_{\text{kin}} &= \frac{2\hbar v_F}{3\pi} \int_0^\infty 2\pi r dr [-\text{sign}(Z)\pi\rho(r)]^{3/2}, \\ E_{\text{pot}} &= \frac{e^2}{4\pi\epsilon_0} \int_0^\infty 2\pi r dr \frac{Z}{\sqrt{d^2 + r^2}} \rho(r), \\ E_{\text{int}} &= \frac{e^2}{8\pi\epsilon_0} \int d^2\mathbf{r} \int d^2\mathbf{r}' \frac{\rho(\mathbf{r})\rho(\mathbf{r}')}{|\mathbf{r} - \mathbf{r}'|}. \end{aligned} \quad (12)$$

It is convenient to express the induced charge density as

$$\rho(\mathbf{r}) \equiv \frac{\tilde{\rho}(r/d)}{d^2}, \quad (13)$$

where $\tilde{\rho}(x)$ is a dimensionless function. Then the Thomas-Fermi approximation to the energy can be written as²²

$$\begin{aligned} E_{\text{TF}} &= \frac{2\pi e^2 Z}{4\pi\epsilon_0 d} \left[\frac{2}{3\pi Z \alpha_G} \int_0^\infty x dx (-\text{sign}(Z)\pi\tilde{\rho}(x))^{3/2} \right. \\ &\quad + \int_0^\infty dx \frac{x\tilde{\rho}(x)}{\sqrt{1+x^2}} + \\ &\quad \left. + \frac{1}{2Z} \int_0^\infty x dx \int_0^\infty x' dx' \tilde{\rho}(x) \mathcal{F}(x, x') \tilde{\rho}(x') \right]. \end{aligned} \quad (14)$$

Here

$$\mathcal{F}(x, x') = \frac{E_K \left[\frac{4xx'}{(x+x')^2} \right]}{x+x'}, \quad (15)$$

and $E_K(x)$ is the complete elliptic integral of the first kind. Ignoring the overall scale of the energy, we realise that the kinetic energy is a small perturbation to the energy. We thus write a perturbation expansion for

$$\tilde{\rho}(x) = \tilde{\rho}_0(x) + \frac{1}{\alpha_G Z} \tilde{\rho}_1(x) + \mathcal{O}\left(\frac{1}{(\alpha_G Z)^2}\right). \quad (16)$$

We substitute this in the Euler-Lagrange equation, and we find an exact solution for ρ_0 ,

$$\tilde{\rho}_0(x) = \frac{-Z}{2\pi(1+x^2)^{3/2}}, \quad (17)$$

which corresponds to a perfect (metallic) image charge. This is due to the fact that have used Coulomb's law with $\epsilon = \epsilon_0$ in the final two terms of Eq. (14).

The next correction is given by the solution to the Fredholm equation

$$|Z| \left(\frac{\pi|Z|}{2\pi(1+x^2)^{3/2}} \right)^{1/2} = -\frac{1}{Z} \int_0^\infty x' dx' \mathcal{F}(x, x') \tilde{\rho}_1(x'), \quad (18)$$

which can probably no longer be solved analytically. Since the Thomas-Fermi approximation is only exact to the lowest order, we need to be slightly suspicious about solutions beyond this

regime. Nevertheless, one way to make progress is to deal with ρ_1 , etc., approximately by employing a variational Ansatz with an effective screening factor Z_{TF} ,

$$\rho(x) = \frac{-Z_{\text{TF}}}{2\pi(1+x^2)^{3/2}}, \quad (19)$$

which gives

$$E_{\text{TF}}(Z_{\text{TF}}) = \frac{\pi e^2}{4\pi\epsilon_0 d} \left[\frac{2\sqrt{2}}{15\pi\alpha_G} |Z_{\text{TF}}|^{3/2} + Z Z_{\text{TF}} + \frac{Z_{\text{TF}}^2}{2} \right]. \quad (20)$$

This energy is minimised for

$$\sqrt{-Z_{\text{TF}}/Z} = -y_{\text{TF}} + \sqrt{y_{\text{TF}}^2 + 1} \quad (21)$$

with

$$y_{\text{TF}} = \frac{\sqrt{2}}{10\pi\alpha_G\sqrt{Z}} \quad (22)$$

Asymptotically, we find

$$-\frac{Z_{\text{TF}}}{Z} \approx 1 - 2y_{\text{TF}} + \mathcal{O}(y_{\text{TF}}^2), \quad y_{\text{TF}} \ll 1. \quad (23)$$

Thus the Thomas-Fermi approximation gives results that are not that different from the RPA approximation, but the effective behaviour has changed from semi-metallic (imperfect image charges) to metallic (perfect image charge).

This similarity between these two approach in 2D materials has been observed before: A related discussion regarding the similarity between linear response and the Thomas-Fermi approximation can be found in the work by Stott and collaborators^{31,32}, who conclude that two dimensions the two are rather similar.

III. BILAYER

The effect of (a set of) charges between a graphene bilayer, similar to the case of a parallel plate capacitor, is of particular interest if we consider van der Waals sandwiches, where the two outer layers are graphene. In this regime we should probably only consider the weak coupling, since we have no unscreened charges. Of course, the Fermi velocity in these outer layers could be rather different, e.g., if one is mounted on a substrate, and the other not.

A. Equal Fermi velocities

Consider a point charge at position $\mathbf{r}_{\parallel 0}$ parallel and distance z_0 perpendicular in between two otherwise identical graphene layers positioned at a distance d . We shall chose the z coordinate of the layers $\pm d/2$, respectively. The two graphene layers experience an electrostatic potential $V_0(\mathbf{r}_{\parallel}, 0) = V_{\text{Coulomb}}(\mathbf{r}_{\parallel} - \mathbf{r}_{\parallel 0}, |z_0 \pm d/2|)$ from this charge, which induces a charge density in the graphene layers (again $V_{\text{tot}} = V_0 + V_{\text{scr}}$). We assume that these layers are thin, and use the linear response approach, thus

$$\chi(\mathbf{r}_{\parallel}, z) = \chi(\mathbf{r}_{\parallel}) (\delta(z - d/2) + \delta(z + d/2)). \quad (24)$$

We again work in von Laue coordinates and as above we evaluate the screening potential in terms of the linear response to the total potential,

$$V_{\text{scr}}(\mathbf{q}_{\parallel}, z) = \frac{e^2}{2\epsilon_0 q_{\parallel}} \chi(\mathbf{q}_{\parallel}) \left(e^{-q_{\parallel}|z-d/2|} V_{\text{tot}}(\mathbf{q}_{\parallel}, d/2) + e^{-q_{\parallel}|z+d/2|} V_{\text{tot}}(\mathbf{q}_{\parallel}, -d/2) \right). \quad (25)$$

After some mathematical manipulations (see appendix) we find that, assuming $|z|, |z_0| \leq d/2$,

$$V_{\text{scr}}(\mathbf{q}_{\parallel}, z) = -x_{\text{RPA}} Z \frac{e^2}{2\epsilon_0 q_{\parallel}} e^{i\mathbf{q}_{\parallel} \cdot \mathbf{r}_{\parallel 0}} \left(e^{-q_{\parallel}(d/2-z)} \left[\delta c_1(q_{\parallel}) e^{-q_{\parallel}(d/2-z_0)} + c_2(q_{\parallel}) e^{-q_{\parallel}(d/2+z_0)} \right] \right. \\ \left. + e^{-q_{\parallel}(d/2+z)} \left[\delta c_1(q_{\parallel}) e^{-q_{\parallel}(d/2+z_0)} + c_2(q_{\parallel}) e^{-q_{\parallel}(d/2-z_0)} \right] \right) \quad (26)$$

$$= Z \frac{e^2}{2\epsilon_0 q_{\parallel}} e^{i\mathbf{q}_{\parallel} \cdot \mathbf{r}_{\parallel 0}} \frac{-\cosh(z+z_0) + e^{-a-q_{\parallel}d} \cosh(z-z_0)}{\sinh(a+q_{\parallel}d)}. \quad (27)$$

Comparing with equivalent expression for the Green's function of a system with two layers with relative permittivity ϵ_r , e.g. in Ref.³³, we see that this is once again correct if we assume Eqs. (9 and (10), and thus

$$a = \ln \left(\frac{\epsilon_r + 1}{\epsilon_r - 1} \right). \quad (28)$$

IV. RESULTS

We now once again look at the interaction of a point dipole placed at vertical position z , with orientation θ relative to the normal. Calculating the interaction energy as an integral over q_{\parallel} , we find that

$$E(z, \theta) = -\frac{1}{2} D^2 \int dq_{\parallel} q_{\parallel}^2 \text{csch}(a + dq_{\parallel}) \left((\cos^2 \theta + 1) \cosh(2zq_{\parallel}) + e^{-a-dq_{\parallel}} (3 \cos^2 \theta - 1) \right) \\ = -\frac{D^2}{4d^3} \left\{ \frac{1}{2} \frac{\epsilon_r - 1}{\epsilon_r + 1} \left[\Phi \left(\left(\frac{\epsilon_r - 1}{\epsilon_r + 1} \right)^2, 3, \frac{1}{2} - \frac{z}{d} \right) + \Phi \left(\left(\frac{\epsilon_r - 1}{\epsilon_r + 1} \right)^2, 3, \frac{1}{2} + \frac{z}{d} \right) \right] (\cos^2 \theta + 1) \right. \\ \left. + \text{Li}_3 \left(\left(\frac{\epsilon_r - 1}{\epsilon_r + 1} \right)^2 \right) (3 \cos^2 \theta - 1) \right\}.$$

Here $\Phi(z, s, a)$ is the Hurwitz-Lerch transcendental function, and $\text{Li}_3(z)$ is the polylogarithm function. This shows that it is energetically favourable for the dipole to be perpendicular to the surface; also, the central position is an unstable position, and the dipole would like to move close to the surface. For a centrally placed dipole we find, by writing

$$E = -\frac{D^2}{16\pi\epsilon_0 d^3} (c_0(\epsilon_r) + c_2(\epsilon_r) \cos^2 \theta), \quad (29)$$

the results shown in Fig. 1.

The prefactor $D^2/(16\pi\epsilon_0 d^3)$ takes the value 4.27 meV for water (using $D = 1.8546 \pm 0.0006$ Debye units (10^{-18} esu cm)³⁴ and $d = 5$ Å; The attraction associated with perpendicular alignment is 51 meV in the metallic regime, and 29 meV for $\epsilon_r = 5$.

There are a couple of recent experimental results where the dipole force will play an important role. The first of these is the confinement of water between two graphene layers³, which will be

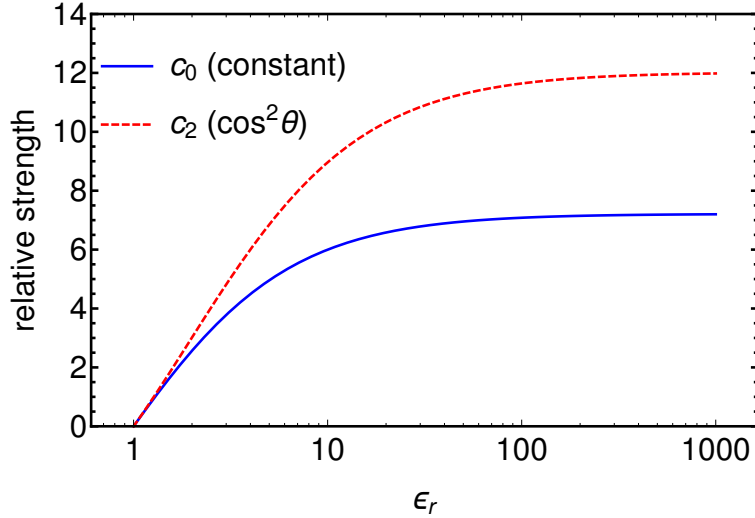


FIG. 1. (Colour online) The behaviour of the coefficients of the constant and of the $\cos^2(\theta)$ terms in Eq. (29) as a function of ϵ_r .

discussed in more detail in Ref.³⁵, since other effects are of real importance there. The second, which we will study here, is the flow of water through graphene microchannels^{3,4}. The analysis in that paper suggests a flow that is very different for a very shallow channel; all evidence suggests that in such channels we have an enhanced flow through organised layers, rather than the more mixed Poiseuille flow for deeper channels³⁶. That raises the question whether the dipole force gives rise to more organisation in such layers.

Water will clearly orient if the interaction of a water molecule with the material is stronger than the thermal energy. We see in Fig. 2 that the outside layer of water will most likely direct perpendicular to the graphene layers ($kT \simeq 25$ meV); the other layers will not orient due the interaction of individual water molecules with the graphene, but may once we take into account the dipole interactions between the water molecules in the layers as well. This suggest that it would be important to include the long-range electromagnetic interactions in the simulations.

V. CONCLUSIONS

We have shown that boundary effects can be important in determining the properties of water and other polar molecules confined within graphene layers. We show that both in the weak-field linear response theory and in the strong-coupling regime we have to deal with image charges; the only difference is that for strong fields graphene behaves as a metal.

The interaction between the molecules and graphene can be approximated using an image charge model. We have estimated the strength of the image charges both in the weak and strong coupling limits. We have considered neutral graphene layers. The formalism can easily be extended to the case when graphene is charged. As the polarizability of the graphene layers will increase, our results can be considered a lower bound to the influence of boundary effects.

The graphene layer tends to orient the molecular dipoles in the direction normal to the layer. For molecules at a few angstroms of the layer, the energy associated to the oriented configuration is comparable, or higher, than room temperature. This energy, for the case of water, is also comparable to the molecule-molecule interaction, which, to a large extent, is also of electrostatic

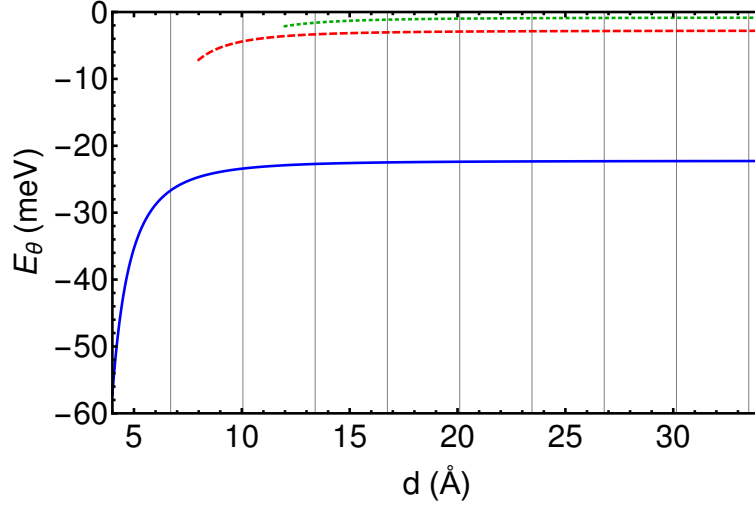


FIG. 2. (Colour online) The energy gain for water approximated as a point dipole placed in a perpendicular orientation in a channel between two graphene layers, as a function of the channel height d . Results are shown for three different distances between the center of the water molecule and one of the graphene layers (blue solid $z = 2$ Å, red dashed $z = 4$ Å, green dotted $z = 6$ Å). The grid lines indicate probable values for the channel height, based on multiples the graphite layer spacing of 3.35 Å.

origin³⁷.

The combination of boundary effects and molecule-molecule interactions, for a single water layer embedded between graphene sheets, will most likely lead to an antiferroelectric arrangement, where the dipoles are oriented in the direction normal to the layers.

VI. ACKNOWLEDGEMENTS

We acknowledge helpful conversations with M. A. Moore and A. K. Geim. F. G. acknowledges financial support from the European Research Council, grant 290846, the European Commission under the contract CNECTICT- 604391, the Graphene Flagship, and MINECO (Spain), grant FIS2014-57432.

Appendix A: Mathematical details

1. Derivation of potential for bilayers

Following from Eq. (25), evaluating the screening potential inside the two layers gives rise to two coupled equations

$$V_{\text{scr}}(\mathbf{q}_{\parallel}, \pm d/2) = -x_{\text{RPA}} \left(V_{\text{scr}}(\mathbf{q}_{\parallel}, \pm d/2) + V_0(\mathbf{q}_{\parallel}, \pm d/2) + e^{-q_{\parallel} d} \left(V_{\text{scr}}(\mathbf{q}_{\parallel}, \mp d/2) + V_0(\mathbf{q}_{\parallel}, \mp d/2) \right) \right), \quad (\text{A1})$$

which we can solve easily:

$$V_{\text{scr}}(\mathbf{q}_{\parallel}, 0 \pm d/2) = c_1(q_{\parallel})V_0(\mathbf{q}_{\parallel}, \pm d/2) + c_2(q_{\parallel})V_0(\mathbf{q}_{\parallel}, \mp d/2), \quad (\text{A2})$$

$$\begin{aligned} c_1(q_{\parallel}) &= -1 + \delta c_1(q_{\parallel}) \\ &= -1 + \frac{e^{q_{\parallel}d}/x_{\text{RPA}}}{2 \sinh(a + q_{\parallel}d)}, \end{aligned} \quad (\text{A3})$$

$$c_2(q_{\parallel}) = -\frac{e^{-a}/x_{\text{RPA}}}{2 \sinh(a + q_{\parallel}d)}, \quad (\text{A4})$$

Here

$$a = \ln \left(\frac{1 + x_{\text{RPA}}}{x_{\text{RPA}}} \right). \quad (\text{A5})$$

Thus

$$V_{\text{tot}}(\mathbf{q}_{\parallel}, 0 \pm d/2) = \delta c_1(q_{\parallel})V_0(\mathbf{q}_{\parallel}, \pm d/2) + c_2(q_{\parallel})V_0(\mathbf{q}_{\parallel}, \mp d/2). \quad (\text{A6})$$

From this we can reconstruct the full potential in momentum space

$$\begin{aligned} V_{\text{scr}}(\mathbf{q}_{\parallel}, z) &= -x_{\text{RPA}} \left(e^{-q_{\parallel}|z-d/2|} V_{\text{tot}}(\mathbf{q}_{\parallel}, d/2) + e^{-q_{\parallel}|z+d/2|} V_{\text{tot}}(\mathbf{q}_{\parallel}, -d/2) \right) \\ &= -x_{\text{RPA}} Z \frac{e^2}{2\epsilon_0 q_{\parallel}} e^{i\mathbf{q}_{\parallel} \cdot \mathbf{r}_{\parallel 0}} \left(e^{-q_{\parallel}|z-d/2|} \left[\delta c_1(q_{\parallel}) e^{-q_{\parallel}|z_0-d/2|} + c_2(q_{\parallel}) e^{-q_{\parallel}|z_0+d/2|} \right] \right. \\ &\quad \left. + e^{-q_{\parallel}|z+d/2|} \left[\delta c_1(q_{\parallel}) e^{-q_{\parallel}|z_0+d/2|} + c_2(q_{\parallel}) e^{-q_{\parallel}|z_0-d/2|} \right] \right). \end{aligned} \quad (\text{A7})$$

2. Unequal Fermi velocities

It is straightforward to generalise these results to two layers with unequal Fermi velocities, e.g., one layer on a substrate and the other free-standing. We introduce the notation x_{\pm} for the value of x_{RPA} for the upper (+) and lower (−) layer, and associate parameters a_{\pm} in a way similar to Eq. (A5). We then find

$$V_{\text{scr}}(\mathbf{q}_{\parallel}, 0 \pm d/2) = c_{1\pm}(q_{\parallel})V_0(\mathbf{q}_{\parallel}, \pm d/2) + c_{2\pm}(q_{\parallel})V_0(\mathbf{q}_{\parallel}, \mp d/2), \quad (\text{A8})$$

$$c_{1\pm}(q_{\parallel}) = -1 + \frac{e^{x_{\mp}/2 + q_{\parallel}d} \sinh(x_{\pm}/2)}{\sinh((a_{+} + a_{-})/2 + q_{\parallel}d)}, \quad (\text{A9})$$

$$c_{2\pm}(q_{\parallel}) = -\frac{e^{x_{\mp}/2} \sinh(x_{\pm}/2)}{\sinh((a_{+} + a_{-})/2 + q_{\parallel}d)}. \quad (\text{A10})$$

* Francisco.Guinea@Manchester.ac.uk

† Niels.Walet@Manchester.ac.uk

¹ A. K. Geim and I. V. Grigorieva, *Nature* **499**, 419 (2013).

² R. R. Nair, H. A. Wu, P. N. Jayaram, I. V. Grigorieva, and A. K. Geim, *Science*, 442 (2012).

³ G. Algara-Siller, O. Lehtinen, F. C. Wang, R. R. Nair, U. Kaiser, H. A. Wu, A. K. Geim, and I. V. Grigorieva, *Nature* **519**, 443 (2015).

- ⁴ M. Neek-Amal, F. M. Peeters, I. V. Grigorieva, and A. K. Geim, *ACS Nano* **10**, 3685 (2016).
- ⁵ E. Khestanova, F. Guinea, L. Fumagalli, A. K. Geim, and I. V. Grigorieva, (2016), arXiv:1604.00086.
- ⁶ A. Mujica, A. Rubio, A. Muñoz, and R. J. Needs, *Rev. Mod. Phys.* **75**, 863 (2003).
- ⁷ S. A. Bonev, E. Schwegler, T. Ogitsu, and G. Galli, *Nature* **431**, 669 (2004).
- ⁸ D. Duan, Y. Liu, F. Tian, D. Li, X. Huang, Z. Zhao, H. Yu, B. Liu, W. Tian, and T. Cui, *Scientific Reports* **4** (2014), 10.1038/srep06968.
- ⁹ N. Bernstein, C. S. Hellberg, M. D. Johannes, I. I. Mazin, and M. J. Mehl, *Physical Review B* **91**, 060511 (2015).
- ¹⁰ I. Errea, M. Calandra, C. J. Pickard, J. Nelson, R. J. Needs, Y. Li, H. Liu, Y. Zhang, Y. Ma, and F. Mauri, *Physical Review Letters* **114**, 157004 (2015).
- ¹¹ J. Chen, G. Schusteritsch, C. J. Pickard, C. G. Salzmann, and A. Michaelides, *Physical Review Letters* **116**, 025501 (2016).
- ¹² F. Corsetti, P. Matthews, and E. Artacho, *Scientific Reports* **6**, 18651 (2016), arXiv: 1502.03750.
- ¹³ R. R. Q. Freitas, R. Rivelino, F. d. B. Mota, and C. M. C. de Castilho, *The Journal of Physical Chemistry A* **115**, 12348 (2011).
- ¹⁴ J. Ma, A. Michaelides, D. AlfÅš, L. Schimka, G. Kresse, and E. Wang, *Physical Review B* **84**, 033402 (2011).
- ¹⁵ E. Voloshina, D. Usvyat, M. SchÅEtz, Y. Dedkov, and B. Paulus, *Physical Chemistry Chemical Physics* **13**, 12041 (2011).
- ¹⁶ X. Li, J. Feng, E. Wang, S. Meng, J. KlimeÅj, and A. Michaelides, *Physical Review B* **85**, 085425 (2012).
- ¹⁷ Y. Wu and N. R. Aluru, *The Journal of Physical Chemistry B* **117**, 8802 (2013).
- ¹⁸ S. McKenzie and H. C. Kang, *Physical Chemistry Chemical Physics* **16**, 26004 (2014).
- ¹⁹ P. Partovi-Azar and T. D. KÅEhne, *physica status solidi (b)* **253**, 308 (2016), arXiv: 1504.04649.
- ²⁰ D. P. DiVincenzo and E. J. Mele, *Phys. Rev. B* **29**, 1685 (1984).
- ²¹ As usual α is the dimensionless coupling constant of QED, $\alpha = e^2/(4\pi\epsilon_0\hbar c) \approx 1/137$.
- ²² M. M. Fogler, D. S. Novikov, and B. I. Shklovskii, *Phys. Rev. B* **76**, 233402 (2007).
- ²³ A. V. Shytov, M. I. Katsnelson, and L. S. Levitov, *Phys. Rev. Lett.* **99**, 246802 (2007).
- ²⁴ V. M. Pereira, J. Nilsson, and A. H. Castro Neto, *Phys. Rev. Lett.* **99**, 166802 (2007).
- ²⁵ A. V. Shytov, M. I. Katsnelson, and L. S. Levitov, *Phys. Rev. Lett.* **99**, 236801 (2007).
- ²⁶ V. N. Kotov, B. Uchoa, V. M. Pereira, F. Guinea, and A. H. Castro Neto, *Rev. Mod. Phys.* **84**, 1067 (2012).
- ²⁷ J. González, F. Guinea, and M. A. H. Vozmediano, *Phys. Rev. B* **59**, R2474 (1999).
- ²⁸ J. D. Jackson, *Classical Electrodynamics*, 3rd ed. (John Wiley & Sons, New York, 1998).
- ²⁹ P. Partovi-Azar and T. D. Kühne, arXiv:1504.04649 [cond-mat, physics:physics, physics:quant-ph] (2015), arXiv: 1504.04649.
- ³⁰ L. Brey and H. A. Fertig, *Phys. Rev. B* **80**, 035406 (2009).
- ³¹ M. Koivisto and M. J. Stott, *Physical Review B* **76**, 195103 (2007).
- ³² L. Calderín and M. J. Stott, *Journal of Physics A: Mathematical and Theoretical* **43**, 155203 (2010).
- ³³ M. Otani and O. Sugino, *Physical Review B* **73**, 115407 (2006).
- ³⁴ S. A. Clough, Y. Beers, G. P. Klein, and L. S. Rothman, *The Journal of Chemical Physics* **59**, 2254 (1973).
- ³⁵ N. R. Walet, (2016), in preparation.
- ³⁶ L. Chan and J. Li, (2016), private communication.
- ³⁷ W. L. Jorgensen, *J. Am. Chem. Soc.* **103**, 335 (1981).